



*universe*

IMPACT  
FACTOR  
**2.9**

CITESCORE  
**3.6**

Review

---

# Loop Quantum Black Hole

---

Xiangdong Zhang

Special Issue

Loop Quantum Gravity and Applications

Edited by


Prof. Dr. Xiangdong Zhang and Dr. Shupeng Song



<https://doi.org/10.3390/universe9070313>

Review

# Loop Quantum Black Hole

Xiangdong Zhang 

Department of Physics, South China University of Technology, Guangzhou 510641, China;  
scxdzhang@scut.edu.cn

**Abstract:** In recent decades, there has been growing interest in the quantization of black holes using techniques developed in loop quantum cosmology. Due to the quantum geometry effect, the resulting quantum-corrected black hole provides non-singular models. The quantization scheme can be roughly divided into four types: (1) the  $\mu_0$  scheme, (2) the  $\bar{\mu}$  scheme, (3) the generalized  $\mu_0$  scheme, and (4) the quantum collapsing model. This paper provides an introduction of the loop quantum black hole model, a summary of the progress made in this field, as well as the quantum effective dynamics and physical applications of these models.

**Keywords:** black hole; loop quantum gravity; singularity resolution

**PACS:** 04.60.Pp; 04.50.Kd

## 1. Introduction

Building a consistent model that unifies quantum mechanics and general relativity (GR) is a Holy Grail for theoretical physicists. Loop quantum gravity (LQG) serves as one of the promising candidates for quantum gravity, which is featured by its non-perturbative characteristics [1–4]. In recent years, LQG has achieved notable progress, including making natural predictions of the discrete geometrical spectrum and providing a reasonable microscopic interpretation to the Hawking–Bekenstein black hole entropy [5–13]. We refer to [13] for a complete review of the results on black hole physics in the framework of loop quantum gravity. This non-perturbative LQG quantization framework has also recently been extended to metric  $f(R)$  theories, Weyl gravity, scalar–tensor theories, higher-dimensional gravity, and so on [14–19]. Despite these remarkable achievements, the LQG dynamics are still not fully understood. In order to understand the dynamics of LQG, one often utilizes symmetry-reduced models to test the quantization technologies developed in full LQG, particularly regarding the Friedmann–Robertson–Walker (FRW) Universe model, leading to the field of loop quantum cosmology (LQC) [20–22]. The most striking feature of LQC is that it can naturally replace the classical Big Bang singularity of the Universe with a quantum bounce, resulting in a nonsingular evolution of the Universe. We refer to [20,23–25] for more complete reviews on LQC.

In addition to Big Bang singularity in cosmological models, another well-known singularity lies at the center of a black hole. For instance, the simplest model is the Schwarzschild interior spacetime, which contains singularity at  $r = 0$ . The interior of a Schwarzschild black hole can be isometric to the Kantowski–Sachs model [22,26]. Thus, the techniques developed for LQC can naturally transport to the spherically symmetric Schwarzschild black hole model. This leads to the field of so-called loop quantum black hole models; we refer to [22,26,27] for detailed constructions of the model. LQC can solve the Big Bang singularity of the Universe. In the loop quantum black hole model, the black hole’s interior singularity can also be resolved, as expected. In [13], concerns were presented about the results on black hole physics in the framework of loop quantum gravity, while in this review, we focus on the loop quantum black hole models utilizing the techniques developed in loop quantum cosmology.



**Citation:** Zhang, X. Loop Quantum Black Hole. *Universe* **2023**, *9*, 313.  
<https://doi.org/10.3390/universe9070313>

Academic Editors: Guillermo A. Mena Marugán and Lorenzo Iorio

Received: 11 April 2023

Revised: 4 June 2023

Accepted: 27 June 2023

Published: 28 June 2023



**Copyright:** © 2023 by the authors. Licensee MDPI, Basel, Switzerland. This article is an open access article distributed under the terms and conditions of the Creative Commons Attribution (CC BY) license (<https://creativecommons.org/licenses/by/4.0/>).

Moreover, in contrast to LQC, which has consistent treatment for various models, in the loop quantum black hole model, different models usually choose different quantum parameters to regularize and quantize the Hamiltonian constraint. Generally, these loop quantum black hole models can be divided into the following four schemes. The first strategy is the  $\mu_o$  scheme. In this scheme, the quantum regularization parameters are set to be constants by certain considerations [22]. The second strategy is the  $\bar{\mu}$  scheme [26,27] with the quantum regularization parameters chosen as functions of the phase space variables. The third is the so-called generalized  $\mu_0$  scheme [28]. The fourth type is the quantum collapsing model [29]. Although the singularity resolution of the Schwarzschild interior holds in both of these methods, the detailed construction of the effective dynamics is quite different. In some schemes, inconsistent physical results will occur. For instance, in  $\mu_o$  scheme, the quantum bounce that replaces the classical singularity of the Schwarzschild interior could appear in the low curvature region [22,30,31]. In  $\bar{\mu}$  scheme, the quantum corrections to the Schwarzschild black hole horizon could be large; however, since the curvature in the horizon is usually very small, one generally believes that the horizon can be considered the classical region and should not receive quantum corrections that are too large [26,27]. To cure these weaknesses, recently, some authors proposed new schemes, the generalized  $\mu_0$  scheme as well as the quantum collapsing model [28,29,32]. Moreover, as suggested by the authors of [33], it is perhaps not suitable to use the  $\bar{\mu}$  scheme near the horizon since a spatial coordinate will become null at the horizon. Hence, they suggest implementing the  $\bar{\mu}$  scheme in a set of particular (spatial) coordinates that will not become null at the horizon. By utilizing the areal gauge and Painlevé–Gullstrand coordinates, they obtained a quantum-corrected Schwarzschild metric, which had the correct semi-classical limit [33]. The aim of this paper is, thus, to provide a summary of these progressions as well as the quantum effective dynamics and physical applications of these models.

We organize the paper as follows: We first recall the Hamiltonian framework of the classical Schwarzschild black hole interior in Section 2. We then study the quantum effective dynamics in Section 3, with different types of quantum parameters. The physical applications of the loop quantum black hole are discussed in Section 4. The conclusions and outlooks are summarized in Section 5. Throughout the paper, we work on the convention  $c = 1$ .

## 2. Classical Theory

### 2.1. Preliminaries

The action of GR reads:

$$S = \frac{1}{16\pi G} \int d^4x \sqrt{-g} R. \quad (1)$$

We begin with this action and choose the spatial metric  $q_{ab}$  and its conjugate momentum  $p^{ab}$  as canonical variables. We can cast the whole system into the geometrical dynamics with the Hamiltonian as follows [2]:

$$H_{grav} = \int d^3x (\mathbb{C}_a N^a + CN), \quad (2)$$

where the diffeomorphism and Hamiltonian constraints read

$$\mathbb{C}_a = D^b p_{ab} = 0, \quad (3)$$

$$C = \frac{2\kappa}{\sqrt{q}} \left( p_{ab} p^{ab} - \frac{1}{2} p^2 \right) - \frac{\sqrt{q}}{2\kappa} R = 0, \quad (4)$$

here,  $q$  is the determinant of metric  $q_{ab}$  and  $\kappa = 8\pi G$ . We can further cast this Arnowitt–Deser–Misner (ADM) Hamiltonian formalism into a connection dynamical formalism. By performing the canonical transformation, we introduce  $E_i^a(x) = \sqrt{q} e_i^a$ —with  $e_i^a e^{bi} = q^{ab}$  denoting the densitized triad and  $A_a^j(x)$  denoting the conjugated connection—as the canonical variables. Since we use a triad rather than a metric, the additional Gaussian constraint

$\mathbb{G}_i$  emerges. Moreover, the diffeomorphism and Hamiltonian constraints should also be re-expressed in terms of new variables  $(A_a^j(x), E_i^a(x))$ . Hence, the whole Hamiltonian reads [2]

$$H_{grav} = \int d^3x \left( \mathbb{G}_i \Lambda^i + \mathbb{C}_a N^a + CN \right), \quad (5)$$

where

$$\begin{aligned} \mathbb{G}_i &= \partial_b E_i^b + \epsilon_{ij}^k A_a^j E_k^a = 0, \\ \mathbb{C}_a &= \frac{1}{\kappa\gamma} E_j^b F_{ab}^j = 0, \\ C &= \frac{1}{2\kappa} \frac{E_i^a E_j^b}{\sqrt{q}} \epsilon^{ij}_k \left( F_{ab}^k - (1 + \gamma^2) \epsilon_{mn}^k K_a^m K_b^n \right) = 0, \end{aligned} \quad (6)$$

represent, respectively, the Gaussian, spatial diffeomorphism, and Hamiltonian constraints. Moreover,  $\gamma$  denotes the Immirzi parameter [2]. In addition,  $F_{ab}^i = \partial_a A_b^i - \partial_b A_a^i + \epsilon_{jk}^i A_a^j A_b^k$  and  $K_a^i$  relates to the extrinsic curvature  $K_{ab}$  through  $K_a^i = K_{ab} e^{bi}$ .

Classically, the spherically static solution to GR is the so-called Schwarzschild solution and the spacetime metric reads

$$ds^2 = - \left( 1 - \frac{2GM}{r} \right) dt^2 + \left( 1 - \frac{2GM}{r} \right)^{-1} dr^2 + r^2 d\Omega^2, \quad (7)$$

where  $M$  stands for the Arnowitt–Deser–Misner (ADM) mass of the compact object. When  $2GM > r$ , this solution represents the exterior region of the Schwarzschild spacetime. On the contrary, when  $2GM < r$ , the Schwarzschild interior metric reads

$$ds^2 = - \left( \frac{2GM}{r} - 1 \right)^{-1} dr^2 + \left( \frac{2GM}{r} - 1 \right) dx^2 + r^2 d\Omega^2. \quad (8)$$

In this case, the killing vector  $(\frac{\partial}{\partial r})^a$  becomes time-like; hence, we can use the radius  $r$  to represent the evolution. Given the Schwarzschild interior spacetime, it has two well-known singularities, one is the true singularity at  $r = 0$  and the other one is located at  $r = 2GM$ , which can be removed by suitable coordinate transformations.

It is easy to see that in the Schwarzschild spacetime, the homogeneous spatial Cauchy slices  $\Sigma$  possess topology  $\mathbb{R} \times \mathbb{S}^2$ . To manifest this symmetry, one usually introduces the following fiducial metric  $\hat{q}_{ab}$  on Cauchy slices  $\Sigma$

$$\hat{q}_{ab} dx^a dx^b = dx^2 + r^2 d\Omega^2. \quad (9)$$

Here,  $x \in (-\infty, \infty)$ , and  $r_0$  has dimensions of length. Note that in the  $x$  direction, the spatial slice  $\Sigma$  is non-compact. Hence, an elementary cell  $\mathcal{C} \cong (0, L_0) \times \mathbb{S}^2$  with a finite  $L_0$  should be introduced in slice  $\Sigma$ . We then calculate all integrals with respect to this elementary cell rather than the divergent  $x$ -direction to avoid possible divergence problems.

The connection  $A_a^i(x)$  and triad  $E_i^a(x)$  will be greatly simplified due to the symmetry as follows [22]

$$E_i^a \tau^i \partial_a = p_c \tau_3 \sin \theta \frac{\partial}{\partial x} + \frac{p_b}{L_0} \tau_2 \sin \theta \frac{\partial}{\partial \theta} - \frac{p_b}{L_0} \tau_1 \frac{\partial}{\partial \phi}, \quad (10)$$

$$A_a^i \tau_i dx^a = \frac{c}{L_0} \tau_3 dx + b \tau_2 d\theta - b \tau_1 \sin \theta d\phi + \tau_3 \cos \theta d\phi, \quad (11)$$

where  $\tau_i$  is a basis of the  $su(2)$  Lie algebra. The non-vanishing Poisson brackets between canonical variables now read

$$\{p_b, b\} = -G\gamma, \quad \{c, p_c\} = 2G\gamma. \quad (12)$$

With the help of Equations (10) and (11), we can express the curvature  $F_{ab}^i$  and the extrinsic curvature  $K_a^i$  as follows:

$$F_{ab}^i \tau_i dx^a dx^b = \frac{bc}{L_0} \tau_1 d\theta \wedge dx + \frac{bc \sin \theta}{L_0} \tau_2 d\phi \wedge dx + (-b^2 \sin \theta + \sin \theta) \tau_3 d\phi \wedge d\theta, \quad (13)$$

$$\gamma K_a^i \tau_i dx^a = \frac{c}{L_0} \tau_3 dx + b \tau_2 d\theta - b \tau_1 \sin \theta d\phi. \quad (14)$$

The Gaussian  $\mathbb{G}_i$  constraint and spatial diffeomorphism constraint  $\mathbb{C}_a$  vanish automatically. We only need to consider the Hamiltonian constraint. By using Equations (13) and (14), the smeared Hamiltonian constraint (6) now reduces to [34,35]

$$H := \int_{\mathcal{C}} NC = -\frac{1}{2G\gamma} \left( \left( b + \frac{\gamma^2}{b} \right) p_b + 2c p_c \right), \quad (15)$$

here, the lapse function  $N$  is chosen as

$$N = \gamma \operatorname{sgn}(p_b) \frac{\sqrt{|p_c|}}{b}. \quad (16)$$

The spacetime metric with spherical symmetry is then [22]

$$ds^2 = -N^2 dT^2 + \frac{p_b^2}{|p_c| L_0^2} dx^2 + |p_c| d\Omega^2.$$

## 2.2. The Classical Dynamics

By using the Hamilton constraint (15). The equations of motion read

$$\begin{aligned} \dot{p}_c &= 2p_c, \\ \dot{c} &= -2c, \\ \dot{p}_b &= \frac{p_b}{2} \left( 1 - \frac{\gamma^2}{b^2} \right), \\ \dot{b} &= -\frac{1}{2} \left( b + \frac{\gamma^2}{b} \right). \end{aligned} \quad (17)$$

The solutions to the above equations read [34,35]

$$p_c(T) = 4m^2 e^{2T}, \quad (18)$$

$$c(T) = \frac{\gamma L_0}{4m} e^{-2T}, \quad (19)$$

$$p_b(T) = -\left( e^{-T} - 1 \right)^{\frac{1}{2}} 2m L_0 e^T, \quad (20)$$

$$b(T) = \gamma \left( e^{-T} - 1 \right)^{\frac{1}{2}}, \quad (21)$$

where  $\infty < T \leq 0$  is the time corresponding to the lapse  $N = \gamma \operatorname{sgn}(p_b) \frac{\sqrt{|p_c|}}{b}$ .

It is easy to see that  $p_c c$  is a constant of the phase space; therefore, we denote  $p_c c =: mL_0 \gamma$ .

By comparing this solution with the Schwarzschild metric (7), we can identify that  $r = 2me^T$ . Moreover, the singularity is located at  $r = 0$  (or  $T = -\infty$ ) and the black hole horizon is located at  $r = 2m$  (or  $T = 0$ ).

## 3. Quantum Theory

To construct a viable quantum framework for Schwarzschild black holes, we adopt the standard LQC treatment for Schwarzschild black holes, which requires introducing

holonomy corrections. Hence, in this section, we will provide a summary of the main steps and constructions.

The holonomy of an  $SU(2)$  connection  $A_a^i$  is a path-ordering exponential integral along an edge  $e^a$  [2,26]

$$h(A) := \mathcal{P} \exp \int_{e_i} dt A_a^j \tau_j^a, \quad (22)$$

with  $\mathcal{P}$  path-ordering labels.

The effective dynamics of LQC for sharply peaked coherent states are known to provide an excellent approximation to the full quantum dynamics [24]. Although it is currently not fully clear whether the effective dynamics of the loop quantum Schwarzschild black hole model will also provide a good approximation of the full LQG dynamics for Schwarzschild black hole spacetimes, the success of LQC makes people believe that, at least for observables whose relevant physical length scales are much larger than Planck scales, the effective dynamics of the loop quantum Schwarzschild black hole model could also be used as a good approximation to the quantum dynamics of semiclassical states. Based on this expectation, we will mainly focus on the effective theory of the loop quantum black hole model here.

Inspired by LQC, a lot of models on quantum black holes have been proposed to solve the singularity inside the black hole's interior. Generally, [22,36], in the quantum effective Hamiltonian constraint, the holonomy correction is simplified by replacing the components of the Ashtekar connection  $b$  and  $c$  with

$$c \rightsquigarrow \frac{\sin(\delta_c c)}{\delta_c}, \quad b \rightsquigarrow \frac{\sin(\delta_b b)}{\delta_b}, \quad (23)$$

where the quantum corrections are controlled by the quantum parameters  $\delta_c$  and  $\delta_b$  due to the fundamental discreteness of LQG. Thus, the effective Hamiltonian of the loop quantum Schwarzschild black hole can be obtained as follows:

$$H_{\text{eff}} = -\frac{1}{2G\gamma} \left[ \left( \frac{\sin(\delta_b b)}{\delta_b} + \frac{\gamma^2 \delta_b}{\sin(\delta_b b)} \right) p_b + 2 \frac{\sin(\delta_c c)}{\delta_c} p_c \right]. \quad (24)$$

Under different choices of  $\delta_b$  and  $\delta_c$ , the current existing quantization schemes of the loop quantum Schwarzschild black hole can be divided into four main classes [37,38]: (1) The  $\mu_0$  scheme [30,39], (2) the  $\bar{\mu}$  scheme [26,40], (3) the generalized  $\mu_0$  scheme [28,32,34,41], and (4) the quantum Oppenheimer–Snyder collapsing model [29]. In the following, we will discuss these four different models in more detail.

### 3.1. $\mu_0$ scheme

In the  $\mu_0$  scheme, the quantum regularization parameters of  $\delta_b$  and  $\delta_c$  are simply taken as constants of the whole phase space [22]. For instance, in [26], the author takes  $\delta_b = \delta_c = \delta$ . In loop quantum cosmology, the  $\mu_0$  scheme suffers a severe problem; it will lead to a bounce in any value of matter density and, therefore, is unphysical. Moreover, in [42], the authors show that when we consider the black hole formation in the  $\mu_0$  scheme, it will suffer another drawback, which is in the  $\mu_0$  scheme; unless an unacceptable value of the Barbero–Immirzi parameter is used, no trapped surfaces could be formed for a non-singular collapse of a homogeneous dust cloud in the marginally bound case.

In this scheme, a particular LQG-corrected Schwarzschild spacetime should be mentioned. The authors constructed a spherically symmetric spacetime through holonomy correction, known as the self-dual solution of LQG [30,39]. In particular, it has been shown

that this solution is regular and free of any spacetime curvature singularity. The metric of the self-dual spacetime by the usual Schwarzschild coordinates is given by [39]

$$ds^2 = -g(r)dt^2 + f(r)dr^2 + \left(r^2 + \frac{a_0^2}{r^2}\right)d\Omega^2, \quad (25)$$

where

$$g(r) = \frac{(r - r_+)(r - r_-)(r - r_*)}{r^4 + a_0^2}, \quad (26)$$

$$f(r) = \frac{(r + r_+)^2(r^4 + a_0^2)}{(r - r_+)(r - r_-)r^4}. \quad (27)$$

Here,  $r_+ = \frac{2M}{(1+P)^2}$ ,  $r_- = \frac{2MP^2}{(1+P)^2}$  and  $r_* = \sqrt{r_+r_-} = \frac{2MP}{(1+P)^2}$ . Moreover,  $a_0 = \frac{\Delta}{8\pi}$ , with  $\Delta$  being the minimal area predicted by LQG [2] and  $P$  is the regularization parameter that depends on small  $\delta \ll 1$  as

$$P = \frac{\sqrt{1 + \gamma^2\delta^2} - 1}{\sqrt{1 + \gamma^2\delta^2} + 1}. \quad (28)$$

It is clear that when  $a_0 = P = 0$ , the above solution (25) reduces to the Schwarzschild black hole exactly.

### 3.2. $\bar{\mu}$ scheme

Since the  $\mu_0$  scheme is unphysical and would lead to wrong semiclassical behavior, to cure this problem, the more complicated quantization scheme of “improved” dynamics, which is usually referred to as the  $\bar{\mu}$  scheme, was formulated. In this scheme, the quantum parameters  $\delta_b$  and  $\delta_c$  are chosen as adaptive discreteness variables. The  $\bar{\mu}$  scheme’s quantization dynamics were first developed in LQC [24] and later generalized for Kantowski–Sachs models [27].

This  $\bar{\mu}$  quantization scheme usually has two choices for  $\delta_b$  and  $\delta_c$ . The first choice is the so-called  $\bar{\mu}$  scheme with

$$\delta_b = \sqrt{\frac{\Delta}{p_b}} \quad \delta_c = \sqrt{\frac{\Delta}{p_c}}. \quad (29)$$

The second choice is usually referred to as the  $\bar{\mu}'$  scheme, as

$$\delta_b = \sqrt{\frac{\Delta}{p_c}} \quad \delta_c = \sqrt{\frac{\Delta p_c}{p_b}}. \quad (30)$$

Although the  $\bar{\mu}$  and  $\bar{\mu}'$  scheme has some advantages over the  $\mu_0$  scheme, it is still not ideal due to its large quantum correction at the horizon, a region typically expected to have little quantum influence.

However, as suggested by some authors [33], it is perhaps not suitable to use the  $\bar{\mu}$  scheme near the horizon because the spatial coordinate becomes null at the horizon due to the fact that the physical length along that coordinate, in this case, will tend to 0. Hence, the authors suggested implementing the  $\bar{\mu}$  scheme in terms of another set of coordinates that will not become null at the horizon. By maintaining the areal gauge for  $p_c$  in the classical theory and using the Painlevé–Gullstrand coordinates, they obtained a quantum-corrected Schwarzschild metric, as:

$$ds^2 = -f(\tau)d\tau^2 + f^{-1}(\tau)dx^2 + \tau^2d\Omega^2, \quad (31)$$

where  $f(\tau) = 1 - \frac{2GM}{\tau} + \gamma^2 \Delta \frac{4G^2 M^2}{\tau^4}$ . This modified metric has the correct classical limit at a large distance. The quantum correction decays vary rapidly at large distances, and curvature scalars  $R$  are bounded by the Planck scale, which is independent of the black hole mass  $M$  [33]. Moreover, this form of the metric was also obtained by other methods, such as the quantum Oppenheimer–Snyder collapsing model [29].

Moreover, an attractive polymerized black hole [37,43] solution belongs to a specific  $\bar{\mu}$  scheme was constructed recently. In this scheme, the quantum regularization parameters are chosen as

$$\delta_b = \pm \frac{4\lambda_j}{\gamma|p_b|}, \quad \delta_c = \pm \frac{8\lambda_k}{\gamma\sqrt{|p_c|}}, \quad (32)$$

where  $\lambda_j$  and  $\lambda_k$  are the regularization constants that are related to the inverse Planck curvature and the Planck length after rescaling the fiducial cell [43]. This solution leads to quantum extensions of the Schwarzschild black hole. The quantum-corrected Schwarzschild-like metric in this scheme reads [37,43–45],

$$ds^2 = -8AF(r)M^2 dt^2 + \frac{dr^2}{8AM^2 F(r)} + G(r)(d\theta^2 + \sin^2(\theta)d\phi^2). \quad (33)$$

where

$$F(r) = \frac{1}{G(r)} \left( \frac{r^2}{8AM^2} + 1 \right) \left( 1 - \frac{2M}{\sqrt{8AM^2 + r^2}} \right), \quad (34)$$

$$G(r) = \frac{512A^3 M^6 + \left( \sqrt{8AM^2 + r^2} + r \right)^6}{8\sqrt{8AM^2 + r^2} \left( \sqrt{8AM^2 + r^2} + r \right)^3}, \quad (35)$$

here,  $M$  represents the mass of the asymptotic Schwarzschild black hole, and the dimensionless parameter  $A$  is given by  $A = \frac{1}{2}(\lambda_k/M^2)^{2/3}$ . The type of extension applied to the Schwarzschild black hole also allows for a bounce from a black hole to a white hole [37,43]. In addition, to date, the black holes found in the universe typically exhibit rotation. With this in mind, the rotational extensions of (33) through the Newman–Janis algorithm were found by the authors in [44].

### 3.3. Generalised $\mu_0$ Scheme

By considering the weaknesses of  $\mu_0$  and  $\bar{\mu}$  schemes, recently, the authors proposed a new scheme [28,32], which is usually referred to as the Ashtekar–Olmedo–Singh (AOS) approach [28,32,46–48]. The AOS scheme can be regarded as an average of the  $\mu_0$ -type and  $\bar{\mu}$ -type schemes. The quantum regularization parameters  $\delta_b$  and  $\delta_c$  are set to be Dirac observables, i.e.,  $\delta_b$  and  $\delta_c$  are constants along each dynamic trajectory but still may be allowed to vary from one to another. This scheme provides a viable effective description for the Kruskal extension of both the exterior and interior of the Schwarzschild black holes with large mass. The effective dynamics, on the one hand, resolve the interior singularity Schwarzschild black holes in the Planck region, and on the other hand, keep the classical horizon regime unchanged, thus overcoming the drawback of the usual  $\bar{\mu}$  scheme. By requiring the physical area of the transition surface to be the minimal area  $\Delta$ , they fix the  $\delta_b$  as

$$\delta_b = \left( \frac{\sqrt{\Delta}}{\sqrt{2\pi}(\gamma)^2 GM} \right)^{\frac{1}{3}}. \quad (36)$$

Meanwhile,  $\delta_c$  takes

$$\delta_c L_0 = \left( \left( \frac{\Delta}{2\pi} \right)^2 \frac{\gamma}{8GM} \right)^{\frac{2}{3}}. \quad (37)$$



The AOS approach has been generalized to the Janis–Newman–Winicour space-time [35]. In these quantum models, the Kretschmann scalar  $K = \frac{144M^2}{\rho_c^3}$  [28,32] is uniformly bounded as

$$K = R_{abcd}R^{abcd} \leq \frac{768\pi^2}{\gamma^4\Delta^2}. \quad (38)$$

The quantum-corrected Schwarzschild metric in this scheme reads

$$ds^2 = -G(r)dt^2 + F(r)dr^2 + H(r)d\Omega^2, \quad (39)$$

where

$$G(r) = \left(\frac{r}{r_s}\right)^{2\epsilon} \frac{(1 - (\frac{r_s}{r})^{1+\epsilon})(2 + \epsilon + \epsilon(\frac{r_s}{r})^{1+\epsilon})^2((2 + \epsilon)^2 - \epsilon^2(\frac{r_s}{r})^{1+\epsilon})}{16(1 + \epsilon)^4(1 + \frac{\delta_c^2 L_o^2 \gamma^2 r_s^2}{16r^4})}, \quad (40)$$

$$F(r) = \left(1 + \frac{\delta_c^2 L_o^2 \gamma^2 r_s^2}{16r^4}\right) \frac{(\epsilon + (\frac{r}{r_s})^{1+\epsilon}(2 + \epsilon))^2}{((\frac{r}{r_s})^{1+\epsilon} - 1)((\frac{r}{r_s})^{1+\epsilon}(2 + \epsilon)^2 - \epsilon^2)}, \quad (41)$$

$$H(r) = r^2 \left(1 + \frac{\delta_c^2 L_o^2 \gamma^2 r_s^2}{16r^4}\right). \quad (42)$$

Here,  $r_s = 2GM$  denotes the Schwarzschild radius and

$$\epsilon = \sqrt{1 + \gamma^2 \left(\frac{\sqrt{\Delta}}{\sqrt{2\pi}(\gamma)^2 GM}\right)^{2/3}} - 1. \quad (43)$$

When quantum correction vanishes, i.e.,  $\epsilon = \delta_b = \delta_c = 0$ , it is clear that the metric (39) goes back to the Schwarzschild solution. It should be mentioned that this model suffers some criticism [49]; the reply to the criticism can be found in [48].

### 3.4. Quantum Oppenheimer–Snyder Collapsing Model

The gravitational collapse process plays an important role in understanding the formation of black holes. In [29], the authors proposed a quantum Oppenheimer–Snyder gravitational collapse model. First, the interior region,  $M^-$ , consists of a dust ball. This region can be described by the Friedmann–Robertson–Walker (FRW) cosmological model. We can write down the flat FRW cosmological line element as follows:

$$ds_{in}^2 = -d\tau^2 + a^2(\tau)(dr^2 + r^2 d\Omega^2). \quad (44)$$

Consider a constant  $r = r_0$  slice, the induced line element on this slice reads

$$ds_{in}^2 = -d\tau^2 + a^2(\tau)r_0^2 d\Omega^2. \quad (45)$$

For the outside region  $M^+$ , we assume that this stationary metric can be expressed as

$$ds_{out}^2 = -f(r)dt^2 + g^{-1}(r)dr^2 + r^2 d\Omega^2. \quad (46)$$

Again, the induced metric on the constant  $r$  slice reads

$$ds_{out}^2 = -(f\dot{t} - g^{-1}\dot{r}^2)d\tau^2 + r^2(\tau)d\Omega^2, \quad (47)$$

here, a dot denotes the derivative with respect to  $\tau$ . Since the collapse is spherical, the interior of the Schwarzschild BH characterized by the Kantowski–Sachs spacetime, exhibits

isometry. By matching the exterior effective spacetime with the interior, the effective LQC model can describe the interior Kantowski–Sachs spacetime. The authors found that [29]

$$g(r) = 1 - H^2 r^2, \quad (48)$$

where  $H = \frac{\dot{a}}{a}$  is the Hubble parameter. By using the classical Friedmann equation  $H^2 = \frac{8\pi G}{3}\rho$ , we have  $g(r) = 1 - \frac{2GM}{r}$  with  $M = \frac{4\pi}{3}\rho r^3$  denoting the total mass of the collapsing ball. If we consider the LQC-corrected Friedmann equation

$$H^2 = \frac{8\pi G}{3}\rho \left(1 - \frac{\rho}{\rho_c}\right). \quad (49)$$

Then  $g(r) = 1 - \frac{2GM}{r} + \gamma^2 \Delta \frac{4G^2 M^2}{\tau^4}$ , which takes the same form as that in (31). Moreover, this kind of metric is also obtained [50] by investigating the gravitational collapse of a homogeneous Gaussian dust cloud.

#### 4. Physical Applications

At the present stage, although there is no completely satisfactory unique solution, even for the loop quantum-corrected Schwarzschild black hole, many physical applications have already been carried out based on the current version of loop quantum black hole models. This is done especially in quantum-corrected metric formalism, such as quasinormal modes [29,51–53], black hole shadow [29,51], gravitational lens [54], solar system tests [45,55], or even galaxy scale tests for a loop quantum black hole. These physical applications can constrain the quantum parameter and, therefore, help us to confirm or rule out some models. For example, recently, a polymer quantum black hole in a  $\bar{\mu}$  generalized scheme was proposed [43,44]. However, in this model, the quantum parameters cannot be fixed by theoretical considerations. In [45], the solar system test was applied to such a loop quantum black hole model and the quantum parameter could be constrained.

Moreover, the Hawking radiation process was calculated in [56]. It was found that the discrete quantum geometry introduces a correction much smaller than the leading contribution for large black holes. In addition, using the effective metric (39), the resulting Hawking temperature of this quantum-corrected black hole horizon also receives a small quantum correction as [48]

$$T_H = \frac{\hbar}{8\pi K M} \frac{1}{1 + \epsilon_m}, \quad (50)$$

where

$$\epsilon_m = \frac{1}{256} \left( \frac{\gamma \Delta^{1/2}}{\sqrt{2\pi M}} \right)^{\frac{1}{\gamma \Delta^{1/2}}}. \quad (51)$$

#### 5. Discussion and Outlook

We presented a summary of loop quantum Schwarzschild models in this paper, and both the classical and effective quantum dynamics were considered. We presented a brief overview of these topics. We started with the classical Hamiltonian framework of the Schwarzschild black hole spacetime. Then, to provide a better understanding of quantum dynamics, we discussed the quantum effective dynamics with four types of quantum regularization parameters,  $\delta_b$  and  $\delta_c$ . These four types of parameters are commonly used for describing quantum dynamics. All corresponding quantum-corrected models can resolve the singularity inside the Schwarzschild black hole. However, they also exhibit some significant differences. Moreover, we summarized the physical applications of these models.

The loop quantum black hole field is still in its infancy stage, unlike LQC, where one has a unique way to fix the quantum parameters. At the present stage, there is still no

completely satisfactory unique solution, even for a Schwarzschild black hole. Moreover, there are still many open issues in the current paradigm, for example, how does one realize the Hawking radiation in such a loop quantum black hole scenario? Can we resolve the black hole information paradox in the loop quantum gravity setup? Moreover, in loop quantum black hole models, the general covariance of spacetime is often discussed. Some authors stated that covariance cannot be addressed in spherical symmetrical models because of slicing dependence [57]. This is currently still an open issue and is under debate. Some possible general covariance models were constructed [58,59]; comments on these models can be found in [60]. These open questions require a deeper understanding of the loop quantum black hole model.

**Funding:** This work is supported by NSFC, No. 12275087, No. 11775082, and “the Fundamental Research Funds for the Central Universities”.

**Data Availability Statement:** Not applicable.

**Conflicts of Interest:** There is no conflict of interest.

## References

1. Rovelli, C. *Quantum Gravity*; Cambridge University Press: Cambridge, UK, 2004.
2. Thiemann, T. *Modern Canonical Quantum General Relativity*; Cambridge University Press: Cambridge, UK, 2007.
3. Ashtekar, A.; Lewandowski, J. Background independent quantum gravity: A status report. *Class. Quantum Gravity* **2004**, *21*, R53. [\[CrossRef\]](#)
4. Han, M.; Ma, Y.; Huang, W. Fundamental structure of loop quantum gravity. *Int. J. Mod. Phys. D* **2007**, *16*, 1397. [\[CrossRef\]](#)
5. Rovelli, C.; Smolin, L. Discreteness of area and volume in quantum gravity. *Nucl. Phys. B* **1995**, *442*, 593. [\[CrossRef\]](#)
6. Ashtekar, A.; Lewandowski, J. Quantum theory of geometry: I. Area operators. *Class. Quantum Gravity* **1997**, *14*, A55. [\[CrossRef\]](#)
7. Ashtekar, A.; Lewandowski, J. Quantum theory of geometry II: Volume operators. *Adv. Theor. Math. Phys.* **1997**, *1*, 388. [\[CrossRef\]](#)
8. Yang, J.; Ma, Y. New volume and inverse volume operators for loop quantum gravity. *Phys. Rev. D* **2016**, *94*, 044003. [\[CrossRef\]](#)
9. Thiemann, T. A length operator for canonical quantum gravity. *J. Math. Phys.* **1998**, *39*, 3372. [\[CrossRef\]](#)
10. Ma, Y.; Soo, C.; Yang, J. New length operator for loop quantum gravity. *Phys. Rev. D* **2010**, *81*, 124026. [\[CrossRef\]](#)
11. Ashtekar, A.; Baez, J.; Corichi, A.; Krasnov, K. Quantum Geometry and Black Hole Entropy. *Phys. Rev. Lett.* **1998**, *80*, 904. [\[CrossRef\]](#)
12. Song, S.; Li, H.; Ma, Y.; Zhang, C. Entropy of black holes with arbitrary shapes in loop quantum gravity. *Sci. China Phys. Mech. Astron.* **2021**, *64*, 120411. [\[CrossRef\]](#)
13. Perez, A. Black Holes in Loop Quantum Gravity. *Rep. Prog. Phys.* **2017**, *80*, 126901. [\[CrossRef\]](#) [\[PubMed\]](#)
14. Zhang, X.; Ma, Y. Extension of Loop Quantum Gravity to  $f(R)$  Theories. *Phys. Rev. Lett.* **2011**, *106*, 171301. [\[CrossRef\]](#) [\[PubMed\]](#)
15. Zhang, X.; Ma, Y. Loop quantum  $f(R)$  theories. *Phys. Rev. D* **2011**, *84*, 064040. [\[CrossRef\]](#)
16. Zhang, X.; Ma, Y. Loop quantum Brans-Dicke theory. *J. Phys. Conf. Ser.* **2012**, *360*, 012055. [\[CrossRef\]](#)
17. Zhang, X.; Ma, Y. Nonperturbative loop quantization of scalar-tensor theories of gravity. *Phys. Rev. D* **2011**, *84*, 104045. [\[CrossRef\]](#)
18. Bodendorfer, N.; Thiemann, T.; Thurn, A. New variables for classical and quantum gravity in all dimensions: I. Hamiltonian Analysis. *Class. Quantum Gravity* **2013**, *30*, 045001. [\[CrossRef\]](#)
19. Zhang, X.; Yang, J.; Ma, Y. Canonical loop quantization of the lowest-order projectable Horava gravity. *Phys. Rev. D* **2020**, *102*, 124060. [\[CrossRef\]](#)
20. Ashtekar, A.; Bojowald, M.; Lewandowski, J. Mathematical structure of loop quantum cosmology. *Adv. Theor. Math. Phys.* **2003**, *7*, 233. [\[CrossRef\]](#)
21. Yang, J.; Zhang, C.; Zhang, X. Alternative  $k = -1$  loop quantum cosmology. *Phys. Rev. D* **2023**, *107*, 046012. [\[CrossRef\]](#)
22. Ashtekar, A.; Bojowald, M. Quantum geometry and the Schwarzschild singularity. *Class. Quantum Gravity* **2006**, *23*, 391. [\[CrossRef\]](#)
23. Bojowald, M. Loop quantum cosmology. *Living Rev. Rel.* **2005**, *8*, 11. [\[CrossRef\]](#) [\[PubMed\]](#)
24. Ashtekar, A.; Pawłowski, T.; Singh, P. Quantum nature of the Big Bang: Improved dynamics. *Phys. Rev. D* **2006**, *74*, 084003. [\[CrossRef\]](#)
25. Ashtekar, A.; Singh, P. Loop quantum cosmology: A status report. *Class. Quantum Gravity* **2011**, *28*, 213001. [\[CrossRef\]](#)
26. Böhmer, C. G.; Vandersloot, K. Loop quantum dynamics of the schwarzschild interior. *Phys. Rev. D* **2007**, *76*, 104030. [\[CrossRef\]](#)
27. Chiou, D.-W. Phenomenological loop quantum geometry of the schwarzschild black hole. *Phys. Rev. D* **2008**, *78*, 064040. [\[CrossRef\]](#)
28. Ashtekar, A.; Olmedo, J.; Singh, P. Quantum transfiguration of kruskal black holes. *Phys. Rev. Lett.* **2018**, *121*, 241301. [\[CrossRef\]](#) [\[PubMed\]](#)
29. Lewandowski, J.; Ma, Y.; Yang, J.; Zhang, C. Quantum Oppenheimer-Snyder and Swiss Cheese models. *Phys. Rev. Lett.* **2023**, *130*, 101501. [\[CrossRef\]](#)

30. Modesto, L. Loop quantum black hole. *Class. Quantum Gravity* **2006**, *23*, 5587. [[CrossRef](#)]
31. Campiglia, M.; Gambini, R.; Pullin, J. Loop quantization of spherically symmetric midi-superspaces. *Class. Quantum Gravity* **2007**, *24*, 3649. [[CrossRef](#)]
32. Ashtekar, A.; Olmedo, J.; Singh, P. Quantum extension of the kruskal spacetime. *Phys. Rev.* **2018**, *98*, 126003. [[CrossRef](#)]
33. Kelly, J.G.; Santacruz, R.; Wilson-Ewing, E. Effective loop quantum gravity framework for vacuum spherically symmetric spacetimes. *Phys. Rev. D* **2020**, *102*, 106024. [[CrossRef](#)]
34. Corichi, A.; Singh, P. Loop Quantization of the Schwarzschild Interior Revisited. *Class. Quantum Gravity* **2016**, *33*, 055006. [[CrossRef](#)]
35. Zhang, C.; Zhang, X. Quantum geometry and effective dynamics of Janis-Newman-Winicour singularities. *Phys. Rev. D* **2020**, *101*, 086002 [[CrossRef](#)]
36. Gambini, R.; Olmedo, J.; Pullin, J. Quantum Black Holes in Loop Quantum Gravity. *Class. Quantum Gravity* **2014**, *31*, 095009. [[CrossRef](#)]
37. Bodendorfer, N.; Mele, F.M.; Munch, J. Mass and Horizon Dirac Observables in Effective Models of Quantum Black-to-White Hole Transition. *Class. Quantum Gravity* **2021**, *38*, 095002. [[CrossRef](#)]
38. Gan, W.; Santos, N.O.; Shu, F.; Wang, A. Properties of the Spherically Symmetric Polymer Black Holes. *Phys. Rev. D* **2020**, *102*, 124030. [[CrossRef](#)]
39. Modesto, L. Semiclassical Loop Quantum Black Hole. *Int. J. Theor. Phys.* **2010**, *49*, 1649. [[CrossRef](#)]
40. Alesci, E.; Bahrami, S.; Pranzetti, D. Quantum Gravity Predictions for Black Hole Interior Geometry. *Phys. Lett.* **2019**, *797*, 134908. [[CrossRef](#)]
41. Olmedo, J.; Saini, S.; Singh, P. From Black Holes to White Holes: A Quantum Gravitational, Symmetric Bounce. *Class. Quantum Gravity* **2017**, *34*, 225011. [[CrossRef](#)]
42. Li, B.; Singh, P. Does the Loop Quantum  $\mu_0$  Scheme Permit Black Hole Formation? *Universe* **2021**, *11*, 406. [[CrossRef](#)]
43. Bodendorfer, N.; Mele, F.M.; Munch, J. Effective Quantum Extended Spacetime of Polymer Schwarzschild Black Hole. *Class. Quantum Gravity* **2019**, *36*, 195015. [[CrossRef](#)]
44. Brahma, S.; Chen, C.; Yeom, D. Testing Loop Quantum Gravity from Observational Consequences of Nonsingular Rotating Black Holes. *Phys. Rev. Lett.* **2021**, *126*, 181301. [[CrossRef](#)]
45. Liu, Y.; Feng, Z.; Zhang, X. Solar system constraints of a polymer black hole in loop quantum gravity. *Phys. Rev. D* **2022**, *105*, 084068. [[CrossRef](#)]
46. Navascués, B.E.; García-Quismondo, A.; Marugán, G.A.M. Mena Marugan, Hamiltonian formulation and loop quantization of a recent extension of the Kruskal spacetime. *Phys. Rev. D* **2022**, *106*, 043531. [[CrossRef](#)]
47. Navascués, B.E.; García-Quismondo, A.; Marugan, G.A.M. Space of solutions of the Ashtekar-Olmedo-Singh effective black hole model. *Phys. Rev. D* **2022**, *106*, 063516. [[CrossRef](#)]
48. Ashtekar, A.; Olmedo, J. Properties of a recent quantum extension of the Kruskal geometry. *Int. J. Mod. Phys. D* **2020**, *29*, 2050076. [[CrossRef](#)]
49. Bodendorfer, N.; Mele, F.M.; Munch, J. A note on the Hamiltonian as a polymerisation parameter. *Class. Quantum Gravity* **2019**, *36*, 187001. [[CrossRef](#)]
50. Giesel, K.; Han, M.; Li, B.; Liu, H.; Singh, P. Spherical symmetric gravitational collapse of a dust cloud: Polymerized dynamics in reduced phase space. *Phys. Rev. D* **2023**, *107*, 044047. [[CrossRef](#)]
51. Liu, C.; Zhu, T.; Wu, Q.; Jusufi, K.; Jamil, M.; Azreg-Ainou, M.; Wang, A. Shadow and quasinormal modes of a rotating loop quantum black hole. *Phys. Rev. D* **2020**, *101*, 084001. [[CrossRef](#)]
52. del-Corral, D.; Olmedo, J. Breaking of isospectrality of quasinormal modes in nonrotating loop quantum gravity black holes. *Phys. Rev. D* **2022**, *105*, 064053. [[CrossRef](#)]
53. Bouhmadi-Lopez, M.; Brahma, S.; Chen, C.; Chen, P.; Yeom, D. A Consistent Model of Non-Singular Schwarzschild Black Hole in Loop Quantum Gravity and Its Quasinormal Modes. *J. Cosmol. Astropart. Phys.* **2020**, *2020*, 066. [[CrossRef](#)]
54. Fu, Q.; Zhang, X. Gravitational Lensing by a Black Hole in Effective Loop Quantum Gravity. *Phys. Rev. D* **2022**, *105*, 064020. [[CrossRef](#)]
55. Zhu, T.; Wang, A. Observational tests of the self-dual spacetime in loop quantum gravity. *Phys. Rev. D* **2020**, *102*, 124042. [[CrossRef](#)]
56. Gambini, R.; Olmedo, J.; Pullin, J. Hawking radiation from a spherical loop quantum gravity black hole. *Class. Quantum Gravity* **2014**, *31*, 115003. [[CrossRef](#)]
57. Bojowald, M.; Brahma, S.; Reyes, J.D. Covariance in models of loop quantum gravity: Spherical symmetry. *Phys. Rev. D* **2015**, *92*, 045043. [[CrossRef](#)]
58. Gambini, R.; Olmedo, J.; Pullin, J. Towards a quantum notion of covariance in spherically symmetric loop quantum gravity. *Phys. Rev. D* **2022**, *105*, 026017. [[CrossRef](#)]

- 
59. Gambini, R.; Olmedo, J.; Pullin, J. Reply to “Comment on ‘Towards a quantum notion of covariance in spherically symmetric loop quantum gravity’”. *Phys. Rev. D* **2022**, *105*, 108902. [[CrossRef](#)]
  60. Bojowald, M. Comment on “Towards a quantum notion of covariance in spherically symmetric loop quantum gravity”. *Phys. Rev. D* **2022**, *105*, 108901. [[CrossRef](#)]

**Disclaimer/Publisher’s Note:** The statements, opinions and data contained in all publications are solely those of the individual author(s) and contributor(s) and not of MDPI and/or the editor(s). MDPI and/or the editor(s) disclaim responsibility for any injury to people or property resulting from any ideas, methods, instructions or products referred to in the content.